# Performance of Bifacial PV Arrays With Fixed Tilt and Horizontal Single-Axis Tracking: Comparison of Simulated and Measured Data

Djaber Berrian, Joris Libal, Markus Klenk, Hartmut Nussbaumer, and Radovan Kopecek

***Abstract*—Compared with standard monofacial photovoltaic (PV) systems, the simulation of the energy yield of bifacial PV systems is more challenging since the impact of factors such as the installation height, the ground albedo, shadowing of neighbored rows, the diffuse irradiance fraction, and the PV module design is more pronounced. Therefore, many academic institutions as well as companies are currently working on the development of suitable modeling tools that allow an accurate energy yield prediction of bifacial systems. In this article, we present the results of energy-yield simulations of bifacial PV systems with fixed tilt and horizontal single-axis tracking (HSAT) in comparison to their monofacial counterparts using a tool that has been developed at ISC Konstanz. In addition, the simulated data are compared with measured results. The energy yield of fixed tilt bifacial systems is simulated as a function of the number of rows and number of modules in a row as well as a function of the installation height. The simulated data have been compared with measured data obtained using a PV system with continuously changing tilt angels. The accuracy of the simulated data is shown to be from +/−0.1% to +/−4% depending on the tilt angle of the bifacial modules. In addition, the energy yield of bifacial HSAT PV systems have been simulated and compared with measured data for a bifacial HSAT system in Chile. In this comparison, the use of ray tracing instead of the view factor (VF) concept for modeling of the rear irradiance reduced the deviation between simulated and measured gain significantly. Therefore, the approach of using VF-based calculations for the front irradiance and ray tracing for the rear irradiance was then used to evaluate different bifacial system configurations in comparison to monofacial ones. Especially, the influence of a variation of the ground coverage ratio on the energy yield for various monofacial, bifacial fixed tilt, and HSAT systems was studied.**

***Index Terms*—Albedo, bifacial modules, bifacial gain, modeling, prediction, photovoltaic (PV) system, ray tracing, tracking, view factor (VF).**

Manuscript received January 30, 2019; revised May 3, 2019; accepted June 13, 2019. Date of publication August 21, 2019; date of current version October 28, 2019. This work was supported by the EC (Horizon 2020) and in part by the German BMWi (FKZ 0324088A) within the Solar-era.net Project "Bifalo." *(Corresponding author: Djaber Berrian.)*

D. Berrian, J. Libal, and R. Kopecek are with the International Solar Energy Research Center Konstanz e.V., 78467 Konstanz, Germany (e-mail: djaber.berrian@isc-konstanz.de; joris.libal@isc-konstanz.de; radovan.kopecek@isc-konstanz.de).

M. Klenk and H. Nussbaumer are with the Zürcher Hochschule für Angewandte Wissenschaften, 8401 Winterthur, Switzerland (e-mail: kleu@zhaw.ch; nusu@zhaw.ch).

Color versions of one or more of the figures in this article are available online at http://ieeexplore.ieee.org.

Digital Object Identifier 10.1109/JPHOTOV.2019.2924394

## I. Introduction

BIFACIAL solar cells generate electrical current when illuminated from the front as well as from the back side. When making both sides of the solar cell available for light absorption, for instance, by using a glass/glass module (or glass/transparent backsheet) structure, bifacial solar cells can generate significantly higher electrical power compared with their monofacial counterparts [1], [2]. A measure of the enhanced specific energy yield of bifacial compared with monofacial photovoltaic (PV) systems is given by the bifacial gain as

$$\mathrm{BG}(\%) = \left(\frac{y_b - y_m}{y_m}\right) \times 100 \quad (1)$$

where $y_b$ is the specific energy yield (kWh/kWp) of a bifacial PV system and $y_m$ is the specific energy yield (kWh/kWp) of a monofacial PV system.

BG is a parameter, which indicates the relative contribution of the rear-side energy yield of a bifacial module compared with the yield generated by a monofacial module with the same front-side STC power and under the same installation conditions. The kWp values of bifacial modules in (1) are measured for front-side illumination at STC with no light entering from the rear side. More details about indoor measurement of bifacial modules can be found in [3].

Early pilot installations of bifacial PV systems have shown that bifacial gain is a critical parameter, which can change significantly from one location to another and can even be influenced by the system size (stand alone, array) at the same site [4]–[6]. Compared with standard monofacial PV systems, the energy yield of bifacial systems shows a stronger dependency on the height, the row-to-row distance, the ground albedo, self-shadowing, the diffuse irradiance fraction, and the module design. In order to simulate the energy yield and BG of bifacial systems, the amount of irradiance on the back of the module is of decisive importance. In the past, different approaches have been undertaken by various authors to model the amount of irradiance reaching the rear side of a bifacial module. On one hand, view factors (VFs) or configuration factors are a robust and well-known concept in the heat transfer theory. This concept has been used for instance by PVsyst and by other authors [7]–[11]. On the other hand, ray tracing is adopted by some scientists to quantify the rear irradiance perceived by the bifacial module [12], [13]. Finally, regarding empirical modeling, there have been few attempts trying to predict only the bifacial gain and not the absolute energy yield [14], [15]. We also expect to see in the

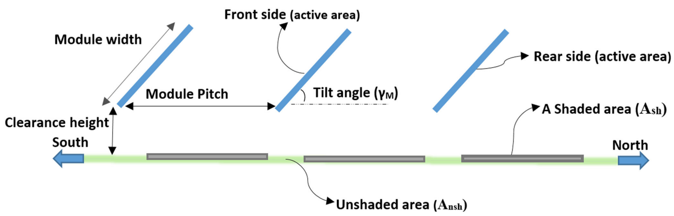


Fig. 1. Schematic representation showing the main geometrical parameters of a fixed tilt, south oriented (i.e., equator oriented for the northern hemisphere) bifacial PV installation: clearance height, module pitch, module tilt, and shaded and unshaded areas.

future machine learning as an alternative approach after accumulating a sufficient amount of field data from bifacial PV plants.

For modeling bifacial HSAT systems, PVsyst 6.7.2 as well as various research institutes [16], [17] are using VFs. In this article, the simulated energy yield and the bifacial gain of fixed tilt and HSAT systems were calculated using VF as well as ray tracing for modeling of the rear-side irradiance. For this purpose, the simulation tool modeling of bifacial distributed gain (MoBiDiG) has been developed at ISC Konstanz and it is under continuous improvement since 2015 [9], [18]. MoBiDiG consists of three main submodels: the optical model (irradiance model), the thermal model, and the electrical model. For fixed tilt and HSAT, a comparison between simulated and experimentally obtained bifacial gains is presented.

## II. MoBiDiG Energy Yield Simulation Model

The rear- and front-side irradiance is composed of three main elements: the direct irradiance, the diffuse irradiance, and the ground reflected irradiance. The detailed description of the irradiance model has been carried out in our previous work [9], [18]. We recall the most important equation in our irradiance model that counts for the ground reflected irradiance seen by the rear side of the bifacial module in order to show the most important dependencies

$$E_{\text{ref,rear}} = \rho \times \text{GHI} \times F_{A_{\text{nsh}} -> A_m} + \rho \times \text{DHI} \times F_{A_{\text{sh}} -> A_m} \tag{2}$$

where $\rho$ is the albedo of the ground surface, GHI is the global horizontal irradiance, and DHI is the diffuse horizontal irradiance.

In Fig. 1, a schematic drawing of a PV system is shown as a side view. Because of the shade beneath the bifacial modules, the model requires a separate calculation of two VFs: the VF from nonshaded areas $F_{A_{\text{nsh}} -> A_m}$ and the VF from shaded areas $F_{A_{\text{sh}} -> A_m}$ to the module back surface. Since the shadow position and shape are changing as a function of time, the VF from the shadow region has to be calculated continuously for each time stamp.

In order to calculate the operating temperature of the PV module, we use the thermal model that requires nominal operating cell temperature NOCT, the plane of array irradiance, and the ambient temperature as inputs [19]. The electrical model is based on a one electrical diode equivalent circuit, which has been solved using the Desoto model [20]. We would like to note that the same thermal and electrical models are defined for both fixed tilt and tracking bifacial PV system.

In order to account for the additional rear irradiance in the electrical model, we define the effective plane of array irradiance

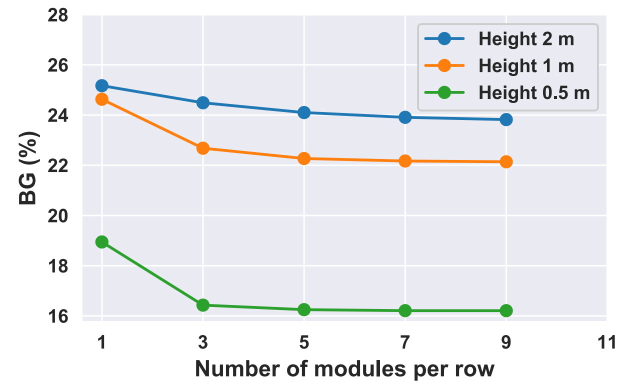


Fig. 2. Bifacial gain of the central module of a single row for fixed-tilt mounting as a function of the number of modules per row. Three different clearance heights of the module are considered.

$E_{\text{eff}}$, which is given by

$$E_{\text{eff}} = E_{\text{Front}} + \varphi \times E_{\text{Rear}} \tag{3}$$

where $\varphi$ is the bifacial factor that is determined as the minimum between the ratio of rear to the front power and rear to front short-circuit current at STC conditions [3].

## III. Simulation of Energy Yield, BG, and Comparison With Measured Data

In the following sections, the simulated energy yields of bifacial fixed tilt and HSAT systems using MoBiDiG are shown and compared with the measured field data.

### A. *Fixed Tilt PV System*

In order to investigate the behavior of fixed tilt bifacial systems, a series of hypothetical scenarios has been modeled using MoBiDiG (using VF for modeling the rear as well as the front-side irradiance). A typical installation configuration of a bifacial fixed tilt, equator-oriented PV system is shown in Fig. 1.

As an example for a hypothetical PV system located in Central Europe, we used as input for the MoBiDiG simulations temperature and irradiance data of one day (15 October 2017) which was provided by Zurich University of Applied Sciences (ZHAW) and which has been collected by the meteorological instrumentation at their test site in Winterthur. In order to define the configuration of the hypothetical PV system, the tilt angle has been fixed to 30° and a constant albedo of 51% has been assumed, whereas for the clearance height, three different values have been investigated: 0.5, 1, and 2 m. In order to investigate the impact of neighboring modules (in the same row) and of neighboring rows on the bifacial gain, we have simulated the power output of the central module (module with lowest rear-side irradiance, worst case scenario) for various total numbers of modules per row and total number of rows. The corresponding simulation results are summarized in Fig. 2 for the various numbers of modules per rows and show clearly that the bifacial gain decreases with increasing number of neighboring modules and with decreasing height.

The decline in bifacial gain with increasing number of modules per row is mainly because of the additional shadow cast by adjacent modules [21]. In addition, we can notice that the BG becomes higher, when the module is higher above the

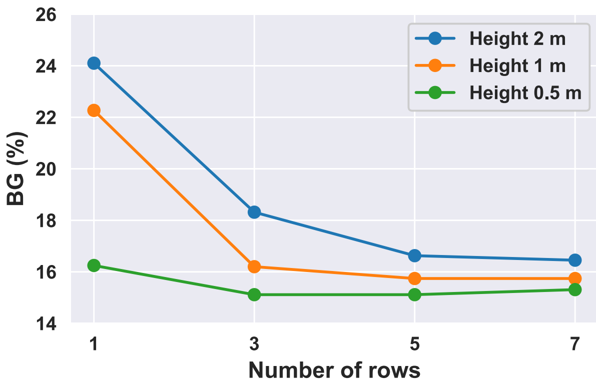


Fig. 3. Bifacial gain of the central module of the central row for fixed-tilt mounting as a function of the number of rows in front and behind the considered row. Three different heights of the module are considered.

ground for the same number of modules per row, as reported by others [22]. The increase of the BG with increasing installation height results from a higher rear-side irradiance caused by a reduced shadowing casted on the ground by the module itself and by neighboring modules as well as the increased capture of diffuse light. However, regardless of the height of the module, a saturation point (five to seven modules per row) is reached, where the bifacial gain of the center module does not decrease further when further increasing the number of modules per row.

A second set of simulations has been performed in order to investigate the effect of neighboring rows on the bifacial gain of the center module. For all simulations with different number of rows, the number of modules per row is set to five, as more modules in a row would not change the result significantly (see Fig. 2). We start with the calculation of the bifacial gain of the central module of a single row then we add, in front of and behind the considered row, an additional module row with the same spacing between the rows [assuming a constant ground coverage ratio (GCR) of 40%] and calculate again the bifacial gain of the new system configuration. This is repeated for 2 and 3 additional rows in front and behind the central row and the result is shown in Fig. 3.

The simulation results in Fig. 3 shows that with increasing number of rows, the BG is decreasing. Each additional row in front and behind the central bifacial module blocks an additional fraction of the ground reflected irradiance seen by the front and back side of the center module. As shown in Fig. 3, the number of rows needed to reach a saturation point depends on the clearance height of the bifacial modules within the row. For instance, at the height of 0.5 m, there is no further diminishing of the bifacial gain if we add a second and a third row behind (and respectively in front of) the considered central row, whereas at the height of 2 m, the rows 2 and 3 can still affect the bifacial gain. In summary, the energy yield of bifacial modules shows a more pronounced dependence on the system size as compared with monofacial PV systems. Experimental setups for measuring the bifacial gain should, therefore, consist of at least 3 modules in a row and minimum 3 rows for installation heights below 0.5 m.

The next step of this article consists in validation of the MoBiDiG tool for fixed-tilt installations. For this aim, we have conducted a comparative analysis using experimental data acquired by the Bifacial Outdoor Rotor Tester (BIFOROT) that is running at ZHAW, Winterthur, Switzerland. In fact, the BIFOROT setup is a new experimental approach to understand and optimize the performance of bifacial PV systems, and it is a useful asset for validating and improving simulation models such as MoBiDiG. The detailed operation of the BIFOROT and its outcomes are reported elsewhere [23]. As depicted in Fig. 4, the BIFOROT consists of three rows with four panels each, oriented full south and permanently revolving, measuring the energy yield of the bifacial module in position M2 at 12 different tilt angles [0°–90°] per minute. It has to be mentioned that the rotation axis of the module rows is in the middle of the modules. The distance between the rotation axis and the ground is indicated as hub height in Table I. Therefore, the clearance height, as indicated in Fig. 1, changes for each tilt angle, which was accounted for in the simulations. All input parameters and meteorological data that are required by MoBiDiG to perform the simulation of the energy yield are measured on the site. The system configuration data important for the simulation are summarized in Table I.

The bar chart in Fig. 5 illustrates the measured, accumulated energy production (kWh) of the bifacial module in position M2 in comparison with simulated data for a period of 5 weeks from October 15, 2017 to November 21, 2017 at different tilt angles. It can be seen that both the modeled and measured energy yield data show a steady increase as a function of the tilt angle from 0° up to 60°. Also for the respective monofacial system, the


Fig. 4. BIFOROT test array at ZHAW, full south oriented in permanent rotation. Measuring the energy yield of the bifacial module in M2 as function of tilt angle from 0° to 90°. Please note that the torque tube is interrupted behind the bifacial PV modules.

TABLE I
USED INSTALLATION CONFIGURATION OF THE BIFOROT FOR COMPARISON WITH SIMULATIONS

| | |
|---|---|
| Albedo (%) | 51 |
| Hub height (m) | 0.75 |
| Module width (m) | 1 |
| Module length (m) | 1.66 |
| GCR (%) | 35 |
| Module tilt angle (°) | Vary |
| Clearance height (m) | Depends on the tilt angle |
| Module azimuth (°) | 180 |

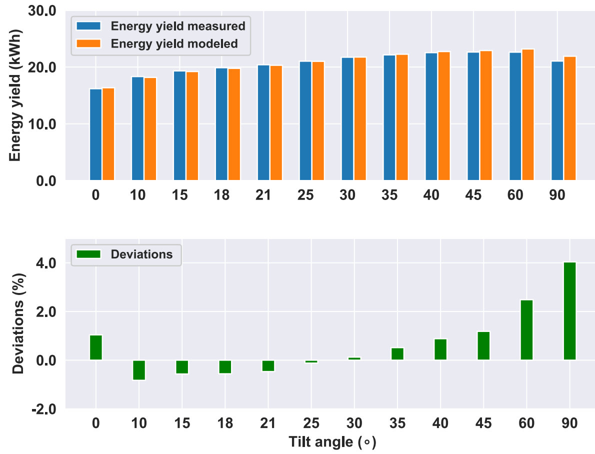


Fig. 5. Measured and modeled accumulated energy yield during five weeks produced by the 270-Wp bifacial module in position M2 at 12 tilt angles. The deviation between measured and modeled data is shown in the lower depiction.

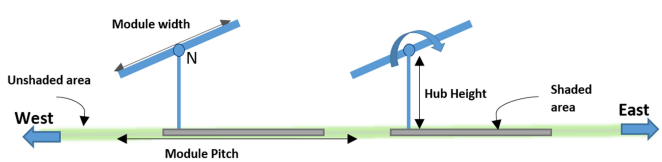


Fig. 6. Schematic representation of the geometrical parameters for a typical horizontal single-axis tracker with a north–south oriented rotation axis.

optimum tilt angle would be expected to be around 60° for the location Winterthur in autumn season.

Overall, there is good agreement between measured and modeled results, except for a relatively high overestimation for steep tilt angles (60° and 90°). The smallest deviation is seen for moderate tilt angles from 10° to 40°.

From the analysis of Fig. 5, it can be expected that, at least for the system configurations studied here, the MoBiDiG model simulates the energy harvest within an accuracy of $+/-1\%$ for any tilt angle in the range of 0° up to 45°.

### B. Horizontal Single-Axis Tracking (HSAT) PV Systems

In this section, we show the results of an investigation about modeling of bifacial HSAT systems. Special attention is given to the influence of the height and of the ground cover ratio on the energy yield. A schematic representation of an HSAT system with a horizontal north–south oriented rotation axis is shown in Fig. 6. Hence, the bifacial HSAT will track the sun from the east toward the west, which will result in a dynamic change of modules tilt angle ($\gamma_M$), whereas its azimuth is toward east before solar noon and toward west after solar noon. The optimum tilt angle $\gamma_M$ for a given timestamp is given when the direction of the sun's irradiance is as close as possible to the perpendicular of the plane of the bifacial module. A detailed description and the mathematical model for the HSAT is given in [24].

Based on our experience and on the results from NREL [21], using the VF concept for the optical modeling leads to an underestimation of the rear-side irradiance when exceeding a certain height of the bifacial module over the ground. For this reason, we perform in this article a comparison between optical modeling by VF and by ray tracing.

TABLE II
INSTALLATION CONFIGURATION FOR THE BASE SCENARIO IN ORDER TO SIMULATE THE BIFACIAL HSAT PV SYSTEM

| Monofacial and Bifacial HSAT | |
|---|---|
| Albedo (%) | 27.5 |
| GCR (%) | 33 |
| Hub height (m) | 2.10 |
| Collector width (m) | 3.75 |
| Axis Azimuth (°) | 0 |
| Tracking Limit Angle (°) | 40 and 60 |

First, we have simulated the front and rear irradiance using NRELs two-dimensional (2-D) open-source VF model, which requires a shorter computation time compared with the quasi 3-D VF model developed at ISC Konstanz and for large-scale PV systems getting similar results compared with the quasi 3-D VF model. In addition, we use bifacial radiance for modeling of the bifacial HSAT system and the simulation tool PVSyst 6.72 for comparison. NRELs bifacial radiance provides some ray tracing (RT) specific functions for front and rear irradiance analysis of a bifacial modules.

As an example for a bifacial HSAT system, La Silla (Chile) has been assumed as installation site. For the following scenarios and for the benchmark (using experimental field data), the meteorological data for this location (La Silla, European South Observatory) has been retrieved from [25] for 4 months of the monitoring time period (September 2016–December 2016). The bifacial PV system in La Silla has been chosen because, to the best of our knowledge, it is up to now—the only large bifacial PV power plant in combination with HSAT, where the minimum required information about the system configuration (GCR, height, ground albedo, and bifacial factor) has been published together with the measured bifacial energy yield gain [26] and at the same time, the hourly irradiance and temperature data monitored at a meteorological station located very close to the PV system site [25]. Therefore, we consider the geometrical parameters of the HSAT PV system for simulations presented in this section as reported in Table II that are identical to La Silla's bifacial tracking PV plant.

In order to reproduce the results of the La Silla's bifacial PV system, we consider a large-scale power plant with solar panel rows of unlimited extend. We also assume an unlimited number of rows and calculate in a first step the optical bifacial gain, which is equivalent to the theoretical maximum obtainable BG for a module with a bifacial factor equal to 1. The optical gain is defined as the ratio of back to front irradiance in percent.

The front-side irradiance as well as the rear irradiance are calculated as a function of tracker axis height using different optical models in order to calculate the optical gain and to determine the best suitable optical model. PVsyst—using a VF concept [27]—and NREL VF are well established methods for modeling of the front-side irradiance (i.e., for monofacial systems). In our simulation, the front irradiance of La Silla PV plant has been modeled by VF and PVsyst 6.7.2, whereas for modeling of the rear side irradiance, ray tracing (RT) has been used in addition to the other methods (VF and PVSyst). The simulation results are summarized in Fig. 7 and are discussed in the following paragraph.

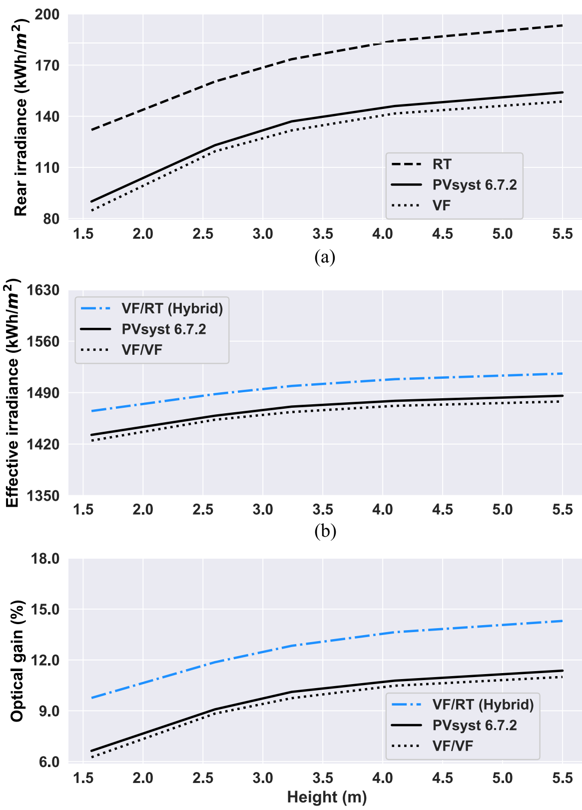


Fig. 7. Comparison of different simulated optical models as a function of the installation height using three different simulation models. (a) Rear irradiance, (b) effective irradiance, and (c) the optical gain of a HSAT bifacial PV system (compared with monofacial HSAT at the same installation configurations) in La Silla. RT and VF stands for ray tracing and view factor, respectively. The combination of different optical models is given by the form: front side/rear side.

While the front-side irradiance is independent from the height (1351.8 kWh/m$^2$ for VF and 1354.8 kWh/m$^2$ for PVSyst) and is, therefore, not shown in Fig. 7, it can be seen [see Fig. 7(a)] that the rear irradiance is increasing with increasing installation height for all models used. Thereby, PVsyst 6.7.2 and VF approaches predict a quite similar amount of rear irradiance as a function of height, whereas the RT model tends to predict much higher irradiance levels on the rear side.

Using the front-side irradiance calculated by VF and rear-side irradiance using the different optical models, we calculate the effective irradiance $E_{\mathrm{eff}}$, as given by (3) and compared them with PVsyst 6.7.2 as follows.

1) *VF/RT (hybrid):* Where the front irradiance is modeled by VF, whereas the rear side by ray tracing.
2) *VF/VF:* The front- and back-side irradiances are modeled by VF.

The results are shown in Fig. 7(b). As the front irradiance is independent on the height, unsurprisingly all models show an increase of the effective irradiance with increasing height and reflect the trend of the rear irradiance calculation [see Fig. 7(a)]. Thus, the VF/RT (hybrid) approach has the highest effective irradiance in comparison with the other approaches.

Finally, the previously calculated values for front- and rear-side irradiances have been used to calculate the optical gain as a function of tracker axis height [see Fig. 7(c)] for the different optical models. Overall, there is a propagation of the trend that has been seen in rear irradiance dependence on height. This means that the optical gain increases as a function of height and the optical hybrid model (VF/RT) shows a higher optical gain than PVsyst 6.7.2 and VF/VF.

TABLE III
MEASURED AND SIMULATED BIFACIAL ENERGY YIELD GAIN OF HSAT BIFACIAL PV SYSTEM (COMPARED WITH MONOFACIAL HSAT AT THE SAME LOCATION) IN LA SILLA FOR FOUR MONTHS OBTAINED USING DIFFERENT MODELS

| HSAT bifacial gain | |
|---|---|
| Measured from [26] | 10.4% - 12.4% |
| Modeled with MoBiDiG Hybrid | 9.3% |
| Modeled with PVsyst 6.7.2 | 6.8% |
| Modeled with MoBiDiG VF | 6.5% |

In order to determine the bifacial energy yield gain, the energy yield of a monofacial and of the equivalent bifacial system have to be calculated. Therefore, the optical model has to be coupled to the thermal and electrical models as described in Section II. In addition to the energy yield calculations by PVsyst, for MoBiDiG, the irradiance data calculated by the two previously described optical models (VF/VF and VF/RT) have been used as input data for the electrical and thermal model.

For the energy yield and bifacial gain analysis, we name MoBiDiG VF and MoBiDiG hybrid if the optical model uses the VF/VF and VF/RT approach, respectively. In order to simulate the bifacial gain for the existing La Silla HSAT PV plant [26], we have run a simulation with a tracking limit angle of 40° (including backtracking) for a tracker axis heights of 2.10 m (see Table II) using MoBiDiG VF, MoBiDiG hybrid, and PVsyst 6.7.2. For a realistic analysis, we have used a bifaciality factor of 85% for the modules, similar to the value obtained for the BiSoN modules used in the La Silla PV plant. As shown, e.g., in [28], for most relevant irradiance conditions, the difference between the operating temperature of monofacial and bifacial modules is less than 1 °C. Accordingly, in the present simulations, it has been assumed that the power loss because of temperature for the monofacial PV module is equal to its bifacial counterpart. The results of these bifacial gain simulations are summarized in Table III.

The bifacial gain for the HSAT PV system simulated by MoBiDiG VF and PVsyst 6.7.2 is below 7% which is significantly below the measured value published in [26]. For the simulated period of four months, we extracted, from the bar chart published in [26], a bifacial gain of 12.4%. As for the La Silla plant, the monofacial reference system is composed of p-type modules, whereas the bifacial modules where nPERT modules (i.e., n-type modules that are not prone to LID), has to be taken into account the LID degradation in the range of 0%–2%. Accordingly, depending on the actual LID that occurred in the monofacial reference module during the monitoring time period, the real bifacial gain might be in between 10.4% and 12.4%. As a result, at least for the system configuration (and meteorological data) studied here, we found that simulating the energy yield with the MoBiDiG hybrid model (using VF for front side and RT for rear-side irradiance modeling) leads to a forecast much closer to the measured data than the models that use the VF optical model for front and rear irradiance. Therefore, for further simulations, only MoBiDiG hybrid had been used as a simulation tool.

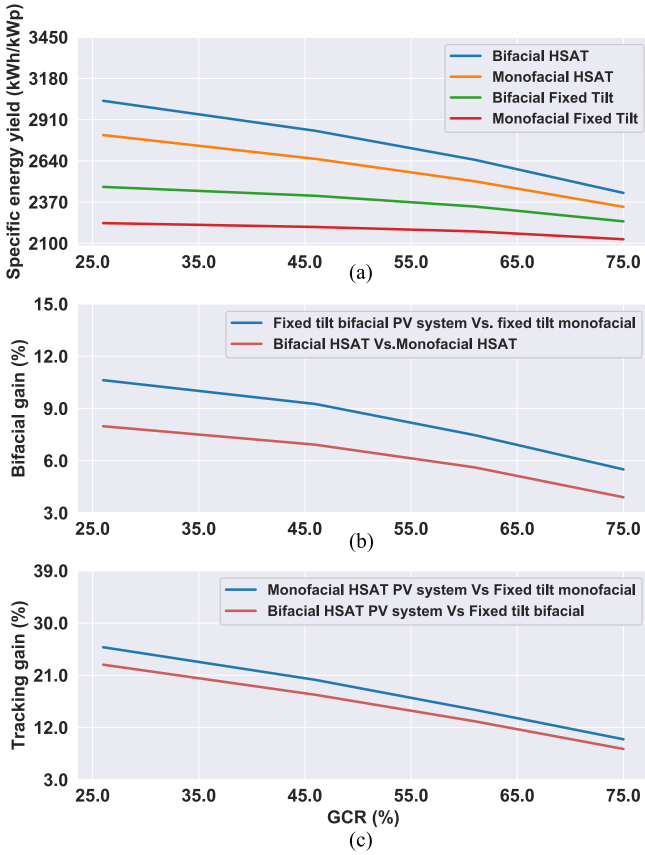


Fig. 8. (a) Simulated full year data plot of the specific energy yield as a function of the ground cover ratio for monofacial and bifacial fixed tilt and HSAT. (b) Bifacial gain of fixed tilt and HSAT PV system as a function of ground cover ratio. (c) Tracking gain for monofacial and bifacial PV system.

### C. Simulated BG as a Function of GCR

For commercial applications, one main purpose of energy yield simulations is to optimize the system design in terms of lowest levelized cost of energy (LCOE). In this context, the area-related balance of system (BOS) cost (land cost and cost of land preparation, cost of module racking, etc.) plays an important role. Accordingly, in this section we simulate the energy yield of hypothetical bifacial and monofacial PV systems in dependence of the ground cover ratio (GCR) using the MoBiDiG hybrid model. All the systems simulated in this section consist of an unlimited number of rows with an unlimited row length.

Fig. 8(a) summarizes the results of these simulations: the simulated specific annual energy yield (kWh/kWp) in dependence from the ground cover ratio (GCR) for monofacial fixed tilt and HSAT systems as well as for their bifacial counterparts. Thereby, the same meteorological data for the La Silla site with the already presented installation parameters (see Table II) have been used as input parameters for the HSAT systems. For the simulation of the fixed-tilt system, the same parameters were used with a tilt angle of 20° (see Table IV).

As also previously reported by Mousel *et al.* [16], it can be seen that the lower the GCR, the higher is the energy yield for all compared PV system types. Furthermore, for a given GCR, the increase in energy yield (bifacial gain) for bifacial compared with monofacial fixed tilt, is higher than the increase obtained when comparing bifacial with monofacial HSAT [see Fig. 8(b)]. We assume that is because of the fact that for a

TABLE IV
INSTALLATION CONFIGURATION FOR THE BASE SCENARIO IN ORDER TO SIMULATE THE BIFACIAL FIXED-TILT PV SYSTEM

| Monofacial and Bifacial Fixed Tilt | |
|---|---|
| Albedo (%) | 27.5 |
| GCR (%) | 33 |
| Collector height (m) | 2.10 |
| Collector width (m) | 3.75 |
| Collector azimuth (°) | 0 |
| Tilt angle (°) | 20 |

fixed-tilt installation, the orientation and height of the bifacial module with respect to the reflective ground surface is always constant. This, in particular in the morning and evening, creates situations where there is a nonshaded area underneath and close to the module rear side. For bifacial HSAT, the module rear side is always directed toward its own shadow where the amount of ground reflected irradiance is lower than for the unshaded areas.

As already mentioned, lowest LCOE is usually the scope of PV system design optimization. Thus, taking into account that typical (i.e., optimized for lowest LCOE) HSAT systems have a GCR of below 35%, whereas fixed systems frequently are implemented with GCR above 50%, comparisons of energy yield or bifacial gains between HSAT and fixed-tilt systems should not be done at the same GCR but between systems with typical GCR values for the respective configuration (HSAT/fixed). Accordingly, with 7%–8%, the BG of HSAT systems with a GCR of 30%–35% is in the same range (8% to 9%) as the BG of fixed tilt systems with a GCR of 50%–55%.

Looking at the tracking gain [see Fig. 8(c)] calculated by comparing the energy yield of a monofacial and bifacial fixed tilt with their tracked (HSAT) counterpart, we can state that, at least for this specific scenario, for a given GCR, the tracking gain for monofacial systems is slightly higher than the tracking gain for bifacial systems.

In general, from Fig. 8(a), it can be observed that the decrease in energy yield with increasing GCR is more pronounced for tracked (HSAT) systems than for fixed systems.

## IV. Conclusion

The energy yield of bifacial fixed tilt and HSAT systems has been simulated using different optical models for the rear-side irradiance. In case of the fixed-tilt systems, the simulated data have been compared with the measured data of a specifically designed test rig (BIFOROT), where the energy output of bifacial modules can be measured at different tilt angles under almost equal illumination conditions. The analysis of a dataset covering a five-week time period in autumn, shows an accuracy of the MoBiDiG VF model of $+/-1\%$ for any angle in the range of 0° to 45°. It has been also found that the BG decreases with increasing system size. Therefore, in order to be relevant for large PV systems, experimental setups for measuring the bifacial gain should consist of at least three modules in a row and minimum three rows for clearance heights below 0.5 m and even larger sized systems are required for clearance heights of above 1 m. The simulations have also confirmed that increasing the mounting height increases the BG for both, large-scale PVsystems as well as for small PV arrays. However, the system size as well as the height have shown a saturation point beyond which a further increase will have no significant impact on bifacial gain. This finding is of particular interest when optimizing the computation time for modeling of large PV systems. The energy yield of HSAT systems has been simulated for one specific plant in La Silla (Chile) using MoBiDiG view factor (VF), MoBiDiG hybrid (VF/RT), and PVsyst 6.7.2 as simulation tools. Thereby, only the innovative MoBiDiG hybrid approach, which models the front irradiance using the VF concept and the rear irradiance with ray tracing, forecasts the bifacial gain with a reasonable accuracy. As the area-related BOS cost has an important impact on the LCOE, using the MoBiDiG hybrid model, the energy yield of several different system configurations were simulated as a function of the GCR. The simulations confirmed that in any case, the use of bifacial instead of monofacial modules leads to significant increases in energy yield no matter if fixed tilt or a HSAT system is used. Accordingly, taking into account that today's state-of-the-art commercial bifacial modules should not cost significantly more as their monofacial counterparts (in particular, bifacial PERC versus monofacial PERC), depending on the specific scenario (characteristics of the location as well as the site specific BOS cost structure), the opportunities to implement bifacial fixed tilt and HSAT systems with lower LCOE than monofacial PV systems are steadily increasing [29]. The results of this article suggest that the VF concept allows for an accurate prediction of the energy yield for bifacial fixed tilt systems, whereas for bifacial HSAT systems, ray tracing is needed for an accurate modeling of the rear-side irradiance and, as a consequence, of the energy yield. Regarding the differences in simulated energy yield using either VF or ray tracing to model the rear side irradiance of bifacial HSAT systems, further work is currently in progress using experimental data that is covering a larger range of system configurations with a particular focus on mounting height. These future studies will contribute to identify the useful application range of VF and ray tracing respectively for rear-side irradiance modeling in order to obtain accurate energy yield predictions for any bifacial PV system by selecting the most appropriate optical model for the respective installation configuration.

## REFERENCES


[1] R. Guerrero-Lemus, R. Vega, T. Kim, A. Kimm, and L. E. Shephard, "Bifacial solar photovoltaics—A technology review," *Renewable Sustain. Energy Rev.*, vol. 60, pp. 1533–1549, 2016. [Online]. Available: http://dx.doi.org/10.1016/j.rser.2016.03.041

[2] D. Berrian, M. Fathi, and M. Kechouane, "Numerical optimization of a bifacial bi-glass thin-film a-Si:H solar cell for higher conversion efficiency," *J. Electron. Mater.*, vol. 47, no. 2, pp. 1140–1150, Feb. 2017. [Online]. Available: http://link.springer.com/10.1007/s11664-017-5828-7

[3] G. Arnoux *et al.*, "Toward the standardisation of the power rating of bifacial solar devices: Technical specification (TS) IEC 60904-1-2," *Presented at the 5th Bifi PV Workshop*, Denver, CO, USA, 2018, pp. 1–20.

[4] L. Kreinin *et al.*, "PV module power gain due to bifacial design. Preliminary experimental and simulation data," in *Proc. 35th IEEE Photovolt. Spec. Conf.*, Jun. 2010, pp. 2171–2175. [Online]. Available: http://ieeexplore.ieee.org/lpdocs/epic03/wrapper.htm?arnumber=5615874

[5] C. Comparotto *et al.*, "Bifacial n-type solar modules: Indoor and outdoor evaluation," in *Proc. 29th Eur. Photovolt. Sol. Energy Conf. Exhib.*, 2014, pp. 3248–3250.

[6] S. Sugibuchi, Koichi, Ishikawa, N, Obara, "Bifacial-PV power output gain in the field test using EarthON high bifaciality solar cells," in *Proc. 28th Eur. Photovolt. Sol. Energy Conf. Exhib.*, 2013, pp. 1–6.

[7] U. A. Yusufoglu *et al.*, "Simulation of energy production by bifacial modules with revision of ground reflection," *Energy Procedia*, vol. 55, pp. 389–395, 2014. [Online]. Available: http://dx.doi.org/10.1016/j.egypro.2014.08.111

[8] A. Krenzinger and E. L. Pigueiras, "Estimation of radiation incident on bifacial albedo-collecting panels," *Int. J. So. Energy*, vol. 4, no. 5, pp. 297–319, 1986.

[9] I. Shoukry and J. Libal, "Master of science thesis bifacial modules-simulation and experiment" Stuttgart Univ., Stuttgart, Germany, Tech. Rep. 2657503, Nov, 2015.

[10] S. M. *et al.*, "PV bifacial yield simulation with a variable Albedo model," in *Proc. EU PVSEC Proc.*, 2016, pp. 1449–1455.

[11] B. Marion *et al.*, "A practical irradiance model for bifacial PV modules," in *Proc. 44th IEEE Photovolt. Spec. Conf.*, 2017, pp. 1537–1542. [Online]. Available: https://www.nrel.gov/docs/fy17osti/67847.pdf

[12] B. Soria, E. Gerritsen, P. Lefillastre, and J.-E. Broquin, "A study of the annual performance of bifacial photovoltaic modules in the case of vertical facade integration," *Energy Sci. Eng.*, vol. 4, no. 1, pp. 52–68, 2016.

[13] C. Reise and A. Schmid, "Realistic yield expectations for bifacial PV systems—An assessment of announced, predicted and observed benefits," in *Proc. 6th PVPMC Workshop*, Freiburg, Germany, 2015. [Online]. Available: https://www.slideshare.net/sandiaecis/42-reise-realisticyieldexpectationsforbifacialpvsystems-56350717

[14] J. E. Castillo-Aguilella and P. S. Hauser, "Bifacial photovoltaic module best-fit annual energy yield model with azimuthal correction," in *Proc. IEEE 44th Photovolt. Spec. Conf.*, Jun., 2017, pp. 1–4.

[15] Solarworld, "Calculating the additional energy yield of bifacial solar modules," 2015, pp. 1–8. [Online]. Available: http://www.solarworld-usa.com/ /media/www/files/white-papers/calculating-additional-energy-yield-through-bifacial-solar-technology-sw9002us.pdf

[16] S. Mousel, E. Lutun, and K. Radouane, "Modelling of single-axis tracking gain for bifacial PV systems," in *Proc. 32nd Eur. Photovolt. Sol. Energy Conf. Exhib.*, 2016, pp. 1610–1617.

[17] M. A. Anoma *et al.*, "View factor model and validation for bifacial PV and diffuse shade on single-axis trackers," in *Proc. 44th IEEE PVSC*, Washington, DC, USA, 2017, pp. 1549–1554

[18] D. Berrian, J. Libal, and S. Glunz, "MoBiDiG: Simulations and LCOE," in *Proc. Bifacial Workshop, Konstanz*, Germany, 2017. [Online]. Available: http://bifipv-workshop.com/index.php?id=konstanz-2017-program

[19] R. G. Ross, Jr., and Smokler, "Flat-plate solar array project: Final report: Volume 6, engineering sciences and reliability," Jet Propulsion Lab., Pasadena, CA, USA, Tech. Rep. NASA-CR-180664.

[20] W. De Soto, S. A. Klein, and W. A. Beckman, "Improvement and validation of a model for photovoltaic array performance," *Sol. Energy*, vol. 80, no. 1, pp. 78–88, 2006.

[21] C. Deline *et al.*, "Bifacial PV performance models: Comparison and field results," in *Proc. BiFiPV Workshop, Konstanz Germany*, 2017. [Online]. Available: http://bifipv-workshop.com/index.php?id=konstanz-2017-program

[22] L. Kreinin, A. Karsenty, D. Grobgeld, and N. Eisenberg, "PV systems based on bifacial modules: Performance simulation vs. design factors," in *Proc. IEEE 43rd Photovolt. Spec. Conf.*, 2016, pp. 2688–2691.

[23] M. Klenk *et al.*, "BIFOROT, bifacial outdoor rotor tester," in *Proc. 3rd B Bifacial PV Workshop Miyazaki*, Miyazaki, Japan, 2016. [Online]. Available: http://bifipv-workshop.com/index.php?id=myazaki-program

[24] E. Lorenzo, L. Narvarte, and J. Muñoz, "Tracking and back-tracking," *Prog. Photovolt., Res. Appl.*, vol. 19, no. 6, pp. 747–753, 2011.

[25] Ministerio de Energia, Gobierno de Chile Explorador Solar, Santiago, Chile. [Online]. Available: http://www.minenergia.cl/exploradorsolar/

[26] F. Bizzarri, G. Leotta, and A. Di Stefano, "La Silla PV plant as a utility-scale side-by-side test for innovative modules technologies," in *Proc. 33rd Eur. Photovolt. Sol. Energy Conf. Exhib.*, Nov. 2017, pp. 1978–1982. [Online]. Available: http://www.eupvsec-proceedings.com/proceedings?paper=44211

[27] A. Mermoud and B. Wittmer, "PVsysts new framework to simulate bifacial systems PVPMC Workshop," in *Proc. PVPMC Workshop*, 2016. [Online]. Available: https://fr.slideshare.net/sandiaecis/pvsysts-new-framework-to-simulate-bifacial-systems

[28] M. W. Lamers *et al.*, "Temperature effects of bifacial modules: Hotter or cooler?" *Sol. Energy Mater. Sol. Cells*, vol. 185, no. Mar., pp. 192–197, 2018.

[29] H. Nussbaumer, M. Klenk, J. Libal, and R. Kopecek, "PV systems with lowest LCOE using bifacial modules state-of-the-art systems and components," in *Proc. PV Tech Power*, 2019, pp. 16–17.